Dose-Response:
An International Journal
July-September 2020:1-11

DOI: 10.1177/1559325820951332
journals.sagepub.com/home/dos
SAGE

Altered Response to Total Body Irradiation of C57BL/6-Tg (CAG-EGFP) Mice

Cuihua Liu[1], Kaoru Tanaka[1], Takanori Katsube[1], Guillaume Varès[2], Kouichi Maruyama[1], Yasuharu Ninomiya[1], Zeenath Fardous[3], Chao Sun[4], Akira Fujimori[1], Stéphanie G. Moreno[5], Mitsuru Nenoi[6], and Bing Wang[1]

Abstract

Application of green fluorescent protein (GFP) in a variety of biosystems as a unique bioindicator or biomarker has revolutionized biological research and made groundbreaking achievements, while increasing evidence has shown alterations in biological properties and physiological functions of the cells and animals overexpressing transgenic GFP. In this work, response to total body irradiation (TBI) was comparatively studied in GFP transgenic C57BL/6-Tg (CAG-EGFP) mice and C57BL/6 N wild type mice. It was demonstrated that GFP transgenic mice were more sensitive to radiation-induced bone marrow death, and no adaptive response could be induced. In the nucleated bone marrow cells of GFP transgenic mice exposed to a middle dose, there was a significant increase in both the percentage of cells expressing pro-apoptotic gene Bax and apoptotic cell death. While in wild type cells, lower expression of pro-apoptotic gene Bax and higher expression of anti-apoptotic gene Bcl-2, and significant lower induction of apoptosis were observed compared to GFP transgenic cells. Results suggest that presence of GFP could alter response to TBI at whole body, cellular and molecular levels in mice. These findings indicate that there could be a major influence on the interpretation of the results obtained in GFP transgenic mice.

Keywords

green fluorescent protein, apoptosis, bone marrow death, adaptive response, ionizing radiation, GFP transgenic mice

Introduction

Since the discovery of green fluorescent protein (GFP), cloning and subsequent expression of the GFP gene in heterologous systems have established GFP as a unique genetic reporter and bioindicator system for use in particular visualizing spatial and temporal patterns of gene expression in a variety of organisms. Groundbreaking achievements have been made in biochemical and medicinal studies using GFP as an invaluable tool, resulting in the 2008 Nobel Prize for Chemistry.[1] Allowing for non-invasive monitoring in living and in paraformaldehyde-fixed cells, nowadays, GFP, its homologues, and some other fluorescent proteins are indispensable in many research fields. Application of GFP as a marker has revolutionized biological research in the last few decades.[2]

As a genetic reporter and a bioindicator (biomarker) system to monitor gene expression and protein localization in living organisms, GFP gains extensive use in a wide range of research fields. The transgenic and gene targeting regimes in the varied lives of organisms have been revolutionized by genetically encoded non-invasive auto-fluorescent markers. Among these, GFP offers several advantages over conventional gene-based reporters, such as lacZ and alkaline phosphatase, due to the fact

[1] National Institute of Radiological Sciences, National Institutes for Quantum and Radiological Science and Technology, Chiba, Japan
[2] Cell Signal Unit, Okinawa Institute of Science and Technology, Okinawa, Japan
[3] Institute of Food and Radiation Biology, Atomic Energy Research Establishment, Bangladesh Atomic Energy Commission, People's Republic of Bangladesh
[4] Institute of Modern Physics, Chinese Academy of Sciences, Lanzhou, People's Republic of China
[5] LRTS—François Jacob Institute of Biology, Fundamental Research Division, Atomic Energy and Alternative Energies Commission, Inserm, Fontenay-aux-Roses Cedex, France
[6] Department of Safety Administration, National Institutes for Quantum and Radiological Science and Technology, Chiba, Japan

Received 07 June 2020; received revised 15 July 2020; accepted 27 July 2020

Corresponding Authors:
Mitsuru Nenoi and Bing Wang, National Institutes for Quantum and Radiological Science and Technology, Chiba 263-8555, Japan.
Emails: nenoi.mitsuru@qst.go.jp; wang.bing@qst.go.jp

that its visualization does not require a chromogenic substrate and can be realized *in vivo*.[3] In laboratory mice, for examples, GFP is used as a vital cell marker to study embryogenesis,[4] combinatorial, double-tagged recombination experiments, chimeras or transplantations.[5] As a fact, studies in biology, physiology, development, pharmacokinetics, oncology and botany have benefited tremendously from the applications of GFP and other fluorescent proteins.[6-13] Furthermore, in vaccine research and development, GFP was incorporated into vector constructions to facilitate the recognition of recombinants.[14]

In radiation biology studies, introduction of GFP as a reporter gene into mammalian cells allows visualization of the modified gene expression levels, signal transduction rates, cell metabolism activities, cell cycle phases and cell death, supplying basic information on the cellular response to ionizing radiation (IR). For examples, M phase cancer cells expressing enhanced GFP-aurora kinase B were used to study the cell cycle progression caused by an X-ray microbeam.[15] GFP transgenic medaka fish *Oryzias latipes* were used in work on the responses of embryonic germ cells to gamma-rays and of thymus to X-rays and Fe heavy ions.[16,17] To determine the potential of UV light as a therapeutic modality for minimal residual cancer, which is a major problem in surgical oncology after apparent tumor curative resection, dual-color cancer cells expressing GFP in the nucleus and red fluorescent protein in the cytoplasm were used in the investigation of the UV light efficacy on the killing of cancer cells.[18] Moreover, to understand radiation risks for humans in space, enhanced GFP (EGFP) was used as a favorable suitability in gene expression studies on the response of mammalian cells to UVC exposure in the International Space Station.[19] EGFP was applied in cellular monitoring of the nuclear factor kappaB pathway for assessing the biological effects of accelerated heavy ions as a model of space environmental radiation conditions.[20] In addition, in some experimental biosystems using lower organisms, application of hydrozoan *Obelia longissima* harboring bioluminescence reaction and introduction of GFP into bacteria *Deinococcus radiodurans* were subjected to evaluation on the biological effects of chronic low-dose beta radiation from tritiated water and in situ real-time evaluation of radiation-responsive promoters.[21,22]

GFP of jellyfish *Aequorea victoria* is an unusual protein with visible absorbance and fluorescence. Unlike other reporters, GFP fluorescence emerges in the absence of substrates or cofactors due to that GFP self-contains a fluorescent p-hydroxybenzylidene-imidazolidinone chromophore in the peptide chains. As the sensitivity of wild-type GFP is below that of standard reporter proteins (i.e., beta-galactosidase) utilizing enzymatic amplification, enhancement of wild-type GFP was achieved by human codon optimization and fluorophore mutation, leading to higher expression levels and brighter fluorescence.[23] GFP was originally believed to be biologically inert and no adverse effects were reported in early studies.[14,24,25] However, recent work has suggested the existence of abnormalities (in terms of cytotoxicity, immunogenicity, and overall function) in cells and animals overexpressing GFP.[26] For example, FVB/N mice expressing transgenic GFP, exhibited dilated cardiomyopathy, earlier death, and altered daily time course of urine, liver and kidney.[27,28] In zebrafish *Danio rerio* overexpressing GFP, embryonic cardiac malfunction was observed as well as a defect in aerobic performance in adults.[29] In cells expressing transgenic GFP, studies showed different baseline of mitochondrial transcript expression in human T-cell line JURKAT cells, proteome modifications in breast cancer cell line, apoptosis in NIH/3T3, BHK-21, Huh-7, and HepG2 cells, protein burden in yeast *Saccharomyces cerevisiae* and myopathy in mouse muscle cells.[30-34] In addition, compared to their wild type counterparts, GFP transgenic cells showed altered response to insults including IR. For example, increased oxidative stress and enhanced sensitivity to cytotoxic drugs in neuroblastoma cell lines and significant difference in transcriptional regulation of the mitochondrial genes after exposure to IR were observed.[3,30,35] Collectively, these results suggest that GFP might behave as a confounder which may affect the interpretation of experimental data.

GFP has been extensively used as reporters, indicators or markers in radiation biology studies on the assumption that it is mostly biologically inert in the experimental systems thus no altered response to radiation would occur or should be considered in GFP transgenic organisms compared to their wild type counterparts. However, considerable evidence has gradually accumulated leading to deepening needs for further clarification on this issue. In this work, we comparatively studied the response of GFP transgenic mice (C57BL/6-Tg (CAG-EGFP)) and their wild type counterpart mice (C57BL/6 N) to X-ray total body irradiation (TBI).

Materials and Methods

Animals

Both C57BL/6-Tg (CAG-EGFP) mice and C57BL/6 N wild-type mice were purchased from SLC, Inc. (Japan). The C57BL/6-Tg (CAG-EGFP) mice were originally produced by Dr. Okabe and colleagues belonging to line 131, one of the so-called "green mice" lines.[25] In the mouse genome the transgene integration chromosomal locus was on chromosome 14 D1.[36] The enhanced green fluorescent protein (EGFP) was expressed by the CAG promoter (pCAGGS-EGFP), and almost all tissues and cells (except erythrocytes and hair) of the animals were fluoresced bright green.[25,37] The mice were reported being normal and healthy.[25] In the present work, the homozygous animals were used and these mice showed no abnormal physical appearance and behavioral abnormalities before exposure to high dose of X-rays. In this paper, the short term "C57BL/6N-GFP" was used to denote "C57BL/6-Tg (CAG-EGFP)." C57BL/6 N wild-type (C57BL/6N-WT) mice were used as the counterparts of the C57BL/6N-GFP mice. Animals were kept under a 12 h light-12 h dark photoperiod, housed in autoclaved cages with sterilized wood chips, and allowed to standard laboratory chow (MB-1, Funabashi Farm Co., Japan) and acidified water (pH $= 3.0 \pm 0.2$) *ad libitum*. Based on the

preliminary trials, in the present work at least 6 mice of both genders were used in each experimental point in the cellular and molecular study. At least 22 mice were used in each experimental group in the 30-day survival test.

All experimental protocols (Experimental Animal Research Plan No. 11-1003-5 and No. 07-1049-15, and Research Plan Using Genetically Modified Organisms No. H19-19) involving mice were reviewed and approved by The Institutional Animal Care and Use Committee of the National Institute of Radiological Sciences, National Institutes for Quantum and Radiological Science and Technology (QST-NIRS), Japan. The experiments were performed in strict accordance with the QST-NIRS Guidelines for the Care and Use of Laboratory Animals.

Irradiation

X-rays were generated with an X-ray machine (Pantak-320 S, Shimadzu, Japan) operated at 200 kVp and 20 mA, using a 0.50 mm Al + 0.50 mm Cu filter. An exposure-rate meter (AE-1321 M, Applied Engineering Inc, Japan) with an ionization chamber (C-110, 0.6 ml, JARP, Applied Engineering Inc, Japan) was used for the dosimetry. The mice held in acryl containers were exposed to total body irradiation (TBI) without anesthesia at room temperature.

Mouse Model for Radiation-Induced Adaptive Response

Radiation-induced adaptive response (RAR) is one of the specific phenomena induced by a priming low dose against a subsequent challenge IR at higher doses. To investigate possible altered response to total body irradiation (TBI) at low and high doses in C57BL/6N-GFP mice at whole body level, an attempt was made to induce a RAR using a mouse model for rescue of bone marrow death (Yonezawa Effect) established by Yonezawa and colleagues.[38] In brief, a priming dose at 0.5 Gy was delivered to the animals on postnatal age of 6 weeks followed by a lethal challenge high dose at 7.5 Gy on postnatal age of 8 weeks. The dose rate was at about 0.30 Gy/min for delivering the priming dose was and 0.90 Gy/min for the challenge dose. A successful induction of RAR was judged as a significant reduced mortality observed in the animals receiving both the priming and challenge doses compared to the animals receiving only the challenge dose in the 30-day survival test.

Collection and Fixation of the Nucleated Bone Marrow Cells

To measure altered response to TBI in C57BL/6N-GFP mice at cellular and molecular levels, gene expression, distribution of cells in the different phases of the cell cycle, and apoptotic cell death were analyzed by flow cytometry in the nucleated bone marrow cells collected from animals exposed to a non-lethal high dose at 4.5 Gy or sham-irradiated at the indicated times. In brief, mice were euthanized by CO_2 asphyxiation 3 h or 6 h after TBI. Both femurs of each mouse were removed and the bone marrow tissues were collected by flushing femurs with phosphate buffered saline free from calcium and magnesium ions (PBS (-)). Single cell suspensions of dissociated nucleated bone marrow cells in PBS (-) were filtered through a 40 μm cell strainer (Corning, Inc, USA) after treating bone marrow tissues with tris-buffered ammonium chloride for the lysis of erythrocytes and washing with PBS (-). The nucleated bone marrow cells were then fixed for at least 24 h with either 1% paraformaldehyde phosphate buffer solution (Wako Pure Chemical Industries, Ltd, Japan) at 4 °C for assessment of gene expression or ice-cold 70% ethanol at -20 °C for measurement of cell cycle distribution and apoptosis.

Flow Cytometric Analysis of Gene Expression, Cell Cycle Distribution and Cell Death

For analysis of gene expression, cells were collected 3 h after TBI, fixed with a paraformaldehyde phosphate buffer solution and washed twice with PBS (-). Cells were then permeabilized in 0.1% Triton X-100 and blocked for 1 h at room temperature with 1% bovine serum albumin to prevent non-specific binding. Then cells were incubated overnight at 4 °C with primary monoclonal antibodies: anti-p53 (PAb122) (Enzo Life Sciences, Inc, USA), anti-p21 (F-5) (Santa Cruz Biotechnology, Inc, USA), anti-Bcl-2 (C2) (Santa Cruz Biotechnology, Inc, USA), or anti-Bax (B-9) (Santa Cruz Biotechnology, Inc, USA), diluted at different concentrations. On the following day, cells were washed twice with PBS (-) followed by a further incubation with a goat anti-mouse IgG (H+L) APC secondary antibody (Southern Biotechnology Associates, Inc. USA) diluted 1:200 in PBS (-) containing 1% bovine serum albumin for 1 h in the dark at room temperature. The control was prepared in an identical way except that primary antibody was replaced by an isotype-specific mouse IgG1 monoclonal antibody (PB100) (Sigma-Aldrich, Japan) to discriminate between specific and non-specific fluorescence for the proteins measured. For analysis of cell cycle distribution and apoptosis (sub G1), cells collected 6 h after TBI and fixed with ethanol were incubated with 30 μg/ml propidium iodide (Sigma-Aldrich, Japan) and 50 μg/ml ribonuclease A (Sigma-Aldrich, Japan) for 30 min at 37°C in the dark. Before flow cytometric analysis, cells were washed and re-suspended in PBS (-). Cell cycle parameters and positively stained cells for protein expression were analyzed using a FACSCalibur flow cytometer (BD Biosciences, Franklin Lakes, NJ, USA) with BD FACStation™ software version 6.1. Total 50,000 cells were analyzed in each sample.

Statistical Analysis

Error propagation formula for subtraction was used to calculate increase in percentage of apoptosis and positive stained cells expressing proteins tested after TBI, and error propagation formula for division was used to calculate the ratio of Bax to Bcl-2. Statistical evaluation of the data was done using Chi-squared test for the 30-day survival, analysis of variance (ANOVA) for

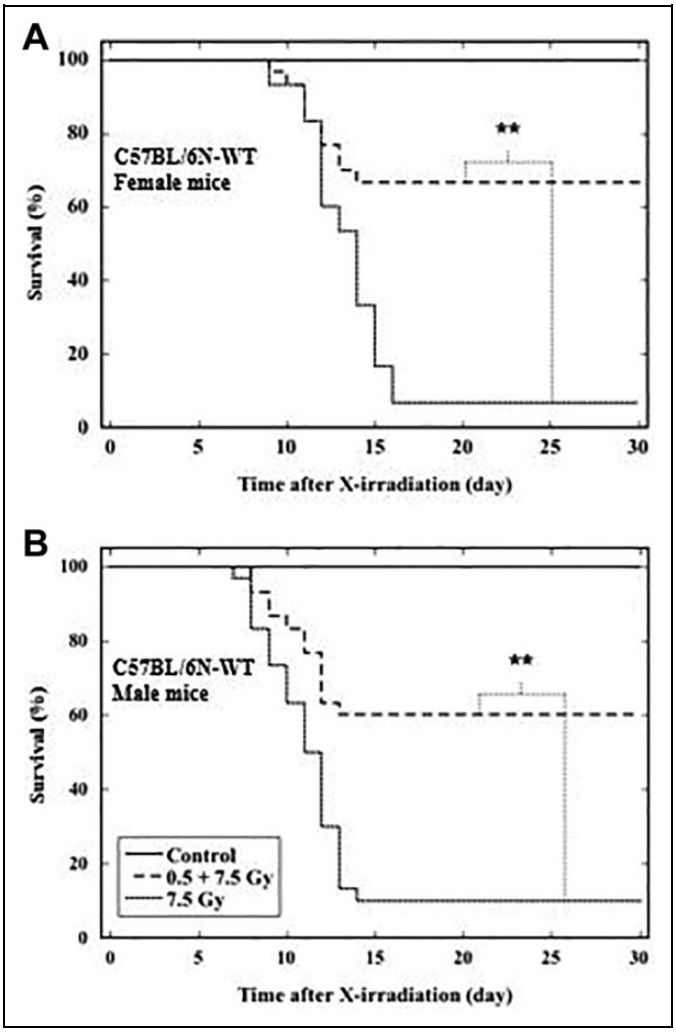

Figure 1. Thirty-day survival test after a challenge dose of 7.5 Gy in C57BL/6N-WT mice. Effect of a priming dose of 0.5 Gy X-rays on a subsequent challenge dose of 7.5 Gy X-rays on mouse 30-day survival was verified in both female (A) and male (B) animals. The solid line denotes the animals (4 females and 4 males) that were untreated with TBI. The dotted line represents the animals (30 females and 30 males) that were irradiated with only the challenge dose at postnatal 8 weeks. The broken line stands for the animals (30 females and 30 males) that were primed with a dose of 0.5 Gy X-rays at postnatal 6 weeks followed by a challenge dose of 7.5 Gy X-rays at postnatal 8 weeks. Two asterisks (**) indicate statistically significant differences ($P < 0.01$) between the 2 groups that were compared.

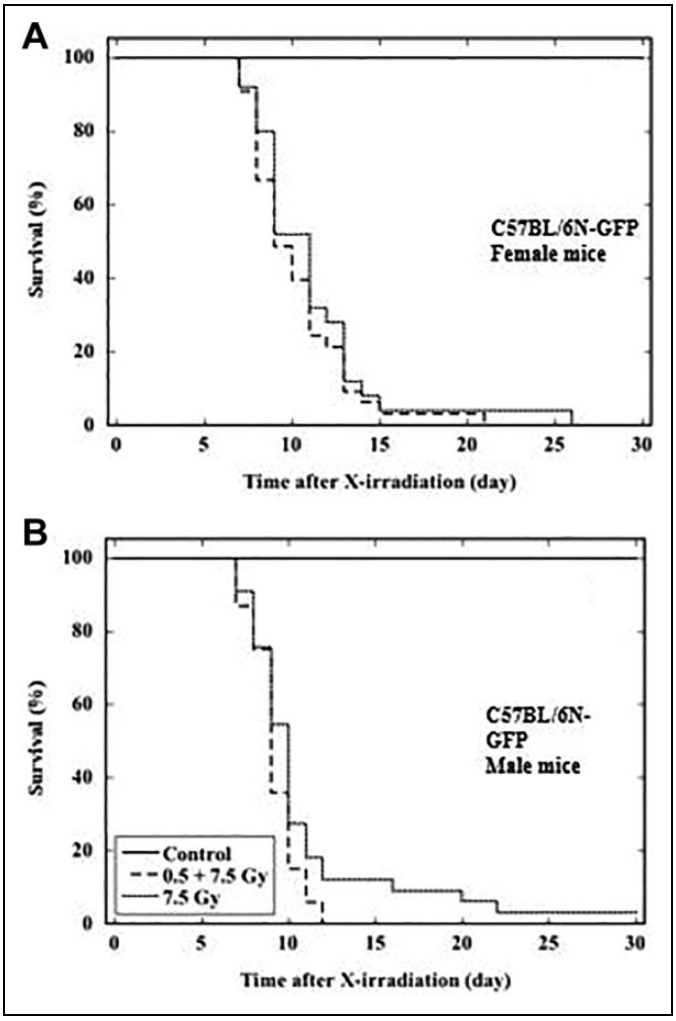

Figure 2. Thirty-day survival test after a challenge dose of 7.5 Gy in C57BL/6N-GFP mice. Effect of a priming dose of 0.5 Gy X-rays on a subsequent challenge dose of 7.5 Gy X-rays on mouse 30-day survival was verified in both female (A) and male (B) animals. The solid line denotes the animals (4 females and 4 males) that were untreated with IR. The dotted line represents the animals (25 females and 33 males) that were irradiated with only the challenge dose at postnatal 8 weeks. The broken line stands for the animals (33 females and 33 males) that were primed with a dose of 0.5 Gy X-rays at postnatal 6 weeks followed by the challenge dose at postnatal 8 weeks. Two asterisks (**) indicate statistically significant differences ($P < 0.01$) between the 2 groups that were compared.

the intergroup differences and Student's *t*-test for the difference between 2 groups for induction of apoptosis and gene expression. The statistical significance was assigned to $P < 0.05$.

Results

Validation of Responses to TBI of C57BL/6N-WT and C57BL/6N-GFP Mice

Responses to TBI at whole body level were studied in C57BL/6N-WT mice (Figure 1) and C57BL/6N-GFP mice (Figure 2) using 30-day survival test as the endpoint. Reproducibility of the RAR mouse model (Yonezawa Effect) in C57BL/6N-WT mice was verified and confirmed in both the females (Figure 1A) and the males (Figure 1B). The survival rate was 66.7% and 60.0% respectively for female and male animals receiving a priming dose of 0.5 Gy X-rays at postnatal 6 weeks followed by a challenge dose of 7.5 Gy X-rays at postnatal 8 weeks. The survival rate was 6.7% and 10.0% respectively for female and male animals receiving only the challenge dose of 7.5 Gy at postnatal 8 weeks. Results showed that administration of the priming dose induced a significant increase in the

survival rate, namely, 60.0% in female and 50.0% in male. These results clearly indicated that RAR was successfully demonstrated in C57BL/6N-WT mice of both genders in our experimental setup.

On the other hand, the survival rate was zero for both female (Figure 2A) and male (Figure 2B) GFP animals receiving a priming dose of 0.5 Gy X-rays followed by a challenge dose of 7.5 Gy X-rays. The survival rate was zero and 3.0% respectively for female and male animals receiving only the challenge dose. Results showed that administration of the priming dose did not induce any increase in the survival rate in both female and male animals. These results clearly indicated that no RAR was demonstrated in C57BL/6N-GFP mice of both genders.

It is noticed that after exposure to TBI at the same lethal dose (7.5 Gy), C57BL/6N-GFP mice appeared more sensitive to IR-induced killing than the C57BL/6N-WT mice, namely, no female animal and 3.0% of male animals survived in the 30-day survival test in C57BL/6N-GFP mice while 6.7% of the females and 10.0% of the males survived in C57BL/6N-WT mice. In addition, most of the death cases occurred either earlier, or in a short period of time in C57BL/6N-GFP mice. For examples, in C57BL/6N-GFP mice receiving the lethal TBI, the first death case occurred on the 7th day for both genders, and 80% death occurred within the 13th day for female and within the 12th day for male animals. While in C57BL/6N-WT mice, the first death case appeared on the 9th day in female and on the 7th day in male animals, and 80% deaths occurred within the 15th day in the females and within the 14th day in the males. Furthermore, to exclude a possibility which the challenge dose at 7.5 Gy was too high to validate existence of RAR in C57BL/6N-GFP mice, 2 lower doses at 7.0 Gy and 6.5 Gy were also tested, and no RAR was induced (data not shown).

All these findings indicated altered response to TBI at both low and high doses at whole body level measured as 30-day survival in C57BL/6N-GFP mice compared to C57BL/6N-WT mice.

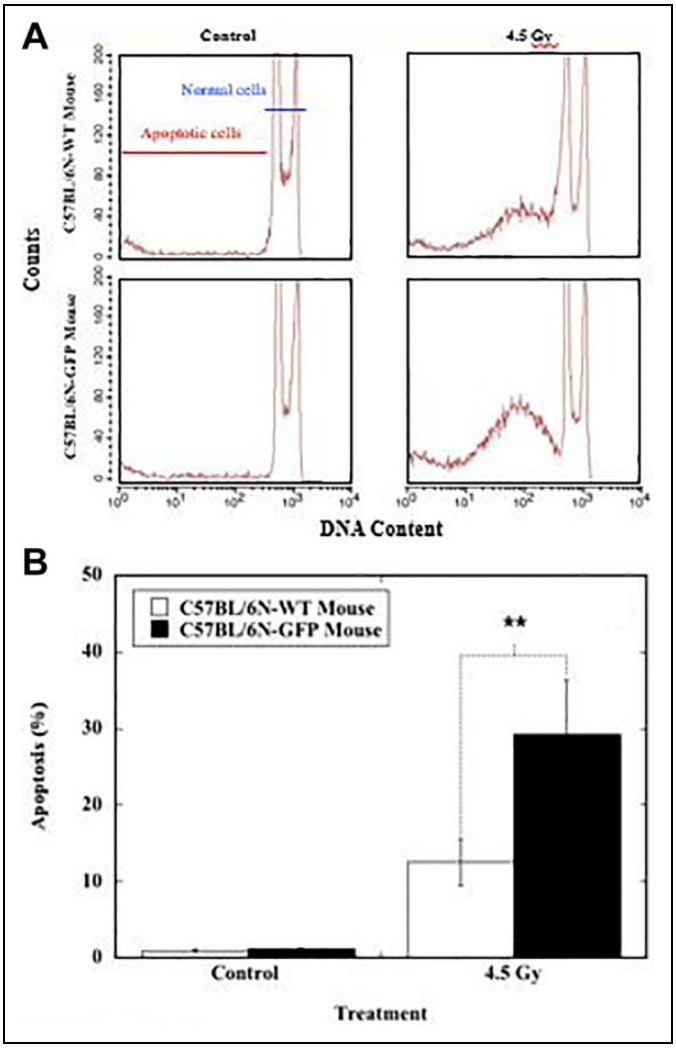

Figure 3. Number of apoptotic cells in the nucleated bone marrow cells in C57BL/6N-WT and C57BL/6N-GFP mice 6 h after 4.5Gy-TBI. Validation of apoptotic cell appearance was performed by flow cytometry. At least 6 samples from both female and male mice were measured at each time point in each group. The representative histogram images were shown in panel A. Results were shown in bar graphs in panel B. Two asterisks (**) indicate statistically significant differences ($P < 0.01$) between the 2 groups that were compared.

Induction of Apoptotic Cells and Change of Cell Cycle Distribution in the Nucleated Bone Marrow Cells After TBI

Percentage of apoptotic nucleated bone marrow cells was analyzed flow cytometrically by measuring cellular DNA content via fluorescent DNA-binding dye propidium iodide. Cells were collected from C57BL/6N-WT and C57BL/6N-GFP mice 6 h after TBI with a nonlethal middle dose at 4.5 Gy (Figure 3). Figure 3A showed some of the representative histogram images obtained in flow cytometry. In the cells from both C57BL/6N-WT and C57BL/6N-GFP mice, background level of apoptosis was very low while it was slightly higher in C57BL/6N-GFP mice. After 4.5 Gy-TBI a significant increase in apoptosis in the cells from both C57BL/6N-WT mice and C57BL/6N-GFP mice, namely, from 1.0% to 12.6% (12.6-fold increase) in C57BL/6N-WT mice and from 1.2% to 29.3% (24.4-fold increase) in C57BL/6N-GFP mice. In addition, a significant decreased bone marrow cellularity (total number of nucleated cells) was observed in both C57BL/6N-WT mice and C57BL/6N-GFP mice while the magnitude of cellularity reduction was markedly higher in C57BL/6N-GFP mice (data not shown). The increase apoptotic fraction in C57BL/6N-GFP mice was markedly higher than that in C57BL/6N-WT mice. These results clearly indicated that significantly increased apoptosis was induced in the nucleated bone marrow cells in both C57BL/6N-WT and C57BL/6N-GFP mice after TBI, and the cells from C57BL/6N-GFP mice were more sensitive to IR-induced cell death compared to that from C57BL/6N-WT mice.

Analysis of cell cycle distribution was performed flow cytometrically by measuring cellular DNA content via fluorescent DNA-binding dye propidium iodide in the nucleated bone

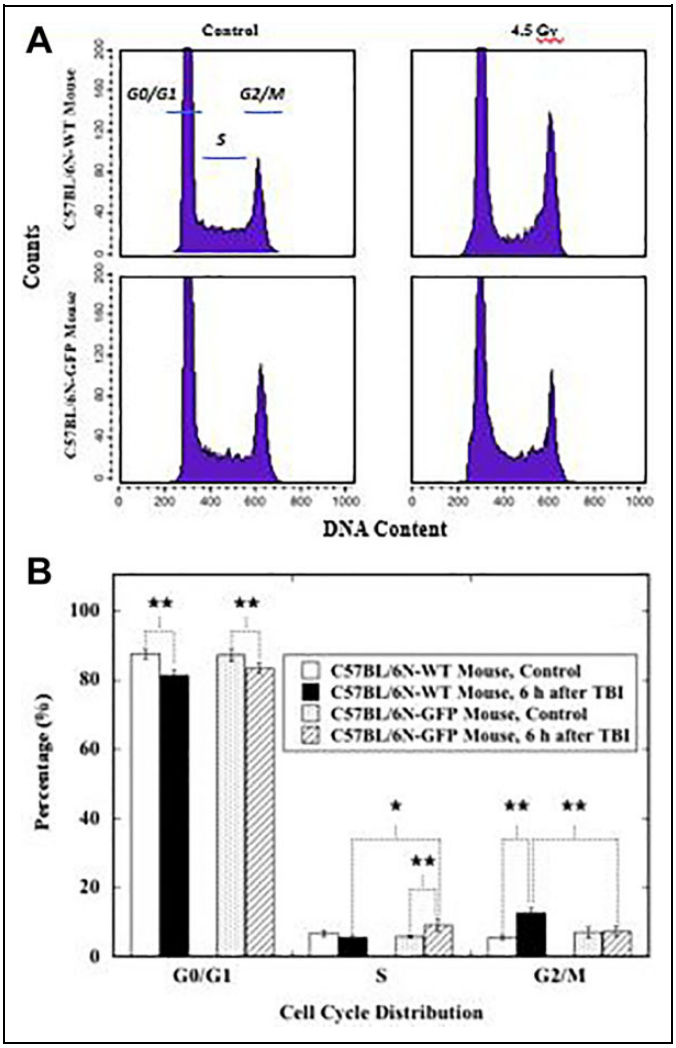

Figure 4. Change of cell cycle phases in the nucleated bone marrow cells in C57BL/6N-WT and C57BL/6N-GFP mice 6 h after 4.5Gy-TBI. Validation of cell cycle phases in the cells was performed by flow cytometry. At least 6 samples from both female and male mice were measured at each time point in each group. The representative histogram images were shown in panel A. Results were shown in bar graphs in panel B. One asterisk (*) and 2 asterisks (**) indicate respectively statistical differences at $P < 0.05$ and $P < 0.01$ between the 2 groups that were compared.

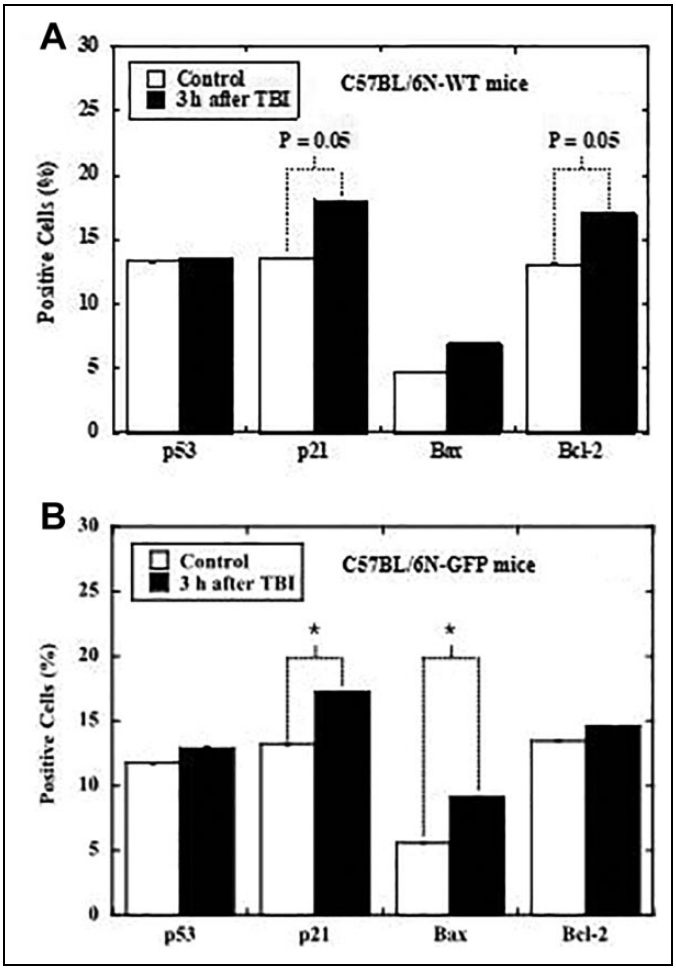

Figure 5. Percentage of positive cells expressing tested proteins in the nucleated bone marrow cells in C57BL/6N-WT (A) and C57BL/6N-GFP (B) mice 3 h after 4.5Gy-TBI. Validation of positive immunohistochemically stained cell appearance in the cells was performed flow cytometrically. At least 6 samples from both female and male mice were measured in each group. One asterisk (*) indicates statistical differences at $P < 0.05$ between the 2 groups that were compared.

marrow cells collected from C57BL/6N-WT and C57BL/6N-GFP mice 6 h after TBI with a nonlethal dose at 4.5 Gy (Figure 4). The representative histogram images were shown in Figure 4A. Without TBI, no significant difference in the distribution of cells in each of cycle phase was observed in both C57BL/6N-WT and C57BL/6N-GFP mice. Six h after TBI, there was a significant decrease in percentage of cells in G0/G1 phase for both C57BL/6N-WT and C57BL/6N-GFP mice. A marked increase was observed in the percentage of S phase cells in C57BL/6N-GFP mice (from 5.8% to 9.1%) and of G2/M phase cells in C57BL/6N-WT mice (from 5.7% to 12.8%). The increase was statistically significant between the cells from C57BL/6N-GFP mice and C57BL/6N-WT mice. These results clearly indicated that TBI induced an S phase arrest in the nucleated bone marrow cells in C57BL/6N-GFP mice and a G2/M phase arrest in C57BL/6N-WT mice.

All these findings indicated altered response to TBI at a moderate dose at cellular level measured as apoptosis and cell cycle distribution in the nucleated bone marrow cells in C57BL/6N-GFP mice compared to that in C57BL/6N-WT mice.

Induction of Cells Expressing Tested Genes in the Nucleated Bone Marrow Cells After TBI

Percentage of positive immunohistochemically stained cells expressing tested genes in the nucleated bone marrow cells from C57BL/6N-WT mice (Figure 5A) and C57BL/6N-GFP mice (Figure 5B) 3 h after TBI was performed flow

cytometrically. Without TBI, the background levels of P53 was slightly higher in the cells from C57BL/6N-WT mice while the background level of Bax was slightly higher in the cells from C57BL/6N-GFP mice. Three hours after TBI, there was a significant increase in the percentage of cells expressing cyclin-dependent kinase inhibitor P21 and Bax in the cells from C57BL/6N-GFP mice. In C57BL/6N-WT mice, increase in the percentage of cells expressing P21 and Bcl-2 was observed and the increase was at the margin of statistical significance ($P = 0.05$).

Of note, the background ratio of Bax to Bcl-2 was 0.42 and 0.37 respectively in the cells from C57BL/6N-GFP mice and their counterparts. After TBI the ratio increased 50.0% to 0.63 in the cells from C57BL/6N-GFP mice and 18.9% to 0.44 in the cells from C57BL/6N-GFP mice and C57BL/6N-WT mice, respectively. These results suggested that in response to TBI at a middle dose, there was a significant higher expression of pro-apoptotic gene Bax in the nucleated bone marrow cells in C57BL/6N-GFP mice while a higher expression of anti-apoptotic gene Bcl-2 in the cells from the C57BL/6N-WT mice.

All these findings indicated alterations at molecular level measured as gene expression in response to TBI at a moderate dose in C57BL/6N-GFP mice compared to the C57BL/6N-WT mice.

Discussion

GFP was discovered in 1961 as a byproduct of the extraction of aequorin from jellyfish *Auquorea Victoria*.[39] While it is one of the most important tools in biology and many transgenic organisms from prokaryotic cells to eukaryotic animals have been developed using GFP technologies, in particular, the EGFP which is one of the engineered variants of the original wild type GFP gene with improved thermostability and fluorescence. To date, *Escherichia coli*, yeast, cultured cells, *Caenorhabditis elegans*, *Drosophila*, butterfly *Junonia orithya*, zebrafish, medaka *Oryzias latipes*, mice, rats, rabbits, lambs, pigs and monkeys are available as GFP transgenic models.[25,40-50] The laboratory mouse is one of the premier mammalian model organisms, and EGFP is popularly used in producing transgenic or targeted mice to create mutations at base pair resolution and tag different cellular populations.[6] Use of GFP and its color variants as reporters and indicators is challenging genome engineering technology and enabling novel approaches in life science studies. On the other hand, application of the GFP transgenic animal models should be verified and considered as these animals could also impose some uncertainties and limitations on their applicability due to alterations in the biological properties and functions compared to their wild type counterparts. It should be also noticed that there is also a possibility that alterations of GFP transgenic animals in the biological properties and functions were not only due to expression of GFP. For example, although the animals looked healthy, integration of GFP plasmid might modify the local chromosome conformation near its locus, directly or indirectly affecting the transcripts of certain genes for important functions such as DNA damage responses. Further work should be done to clarify this point whenever possible using more stains of transgenic animals in which the GFP is located at different genome loci, or with other reliable experimental strategies.

To verify if there are any altered response of GFP transgenic mice to TBI, a mouse model for RAR (Yonezawa Effect) was adopted and applied to this work using C57BL/6N-GFP mice, the first engineered GFP transgenic mice in the world with applications in a wide range of research fields including radiation biology.[25,51-63] RAR is a phenomenon that pre-exposure to a low priming dose reduces the biological effects of a subsequent higher challenge dose. Since the discovery of RAR,[64] it has been demonstrated in a variety of biosystems from simple prokaryotes to higher eukaryotes including mammalian animals with varied endpoints including cell death and bone marrow death.[65-68] The mouse RAR model (Yonezawa Effect) is a well-designed system in investigating response of the mice to IR of both low and high doses using endpoints at molecular, cellular and whole body levels.[38,69-74] There are 2 different phenotypes of RAR in this model involving different mechanisms: the first phenotype could be induced by a low priming dose at 0.30-0.50 Gy leading to radioresistance in blood forming tissues 2 weeks later, and the second phenotype could be induced by a very low priming dose at 0.05-0.10 Gy 2 months later. The model for the first phenotype was used to comparatively study the response in the GFP transgenic mice to TBI with that in their wild type counterparts. GFP transgenic mice showed altered response to the isodose at all endpoints including bone marrow death, induction of adaptive response, and induction of apoptosis and gene expression in the nucleated bone marrow cells.

Taken into consideration the documented studies on changes of biological properties and physiological functions in GFP transgenic cells and animals due mainly to increased reactive oxygen species (ROS) induced by GFP overexpression,[75] ROS may involve at least in a part of the mechanisms underlying alterations in response of GFP transgenic mice to TBI in the present work. ROS are highly reactive molecules, playing important roles in many biological and signaling processes. In a healthy cell there is a balance between generation and neutralization of ROS by endogenous cellular defense machinery, and low levels of ROS inside the cell are required for physiological functioning to regulate signaling mechanisms involved in mitosis and apoptosis. However, when intracellular redox imbalance occurs due to such as excess of ROS production and inefficiency of antioxidant defenses, increased ROS could induce oxidative stress causing structural damage to the surrounding vital cellular molecules, including cytosolic lipids, proteins and DNA. This would lead to dysregulation of physiological functions and increased vulnerability to detrimental health outcomes.[76] Mitochondria are the major source of ROS within a cell and a major target of ROS, subjecting to high levels of ROS-induced damage. Furthermore, damage of enzymes in the electron transport chain of the mitochondria would in turn induce further ROS production.[77] Increased

levels of ROS could induce higher radiosensitivity.[77] In model mice expressing elevated levels of ROS, increased radiosensitivity was demonstrated, which was mediated via dysregulation of antioxidant response and defective redox homeostasis.[69-79] These animals showed increased apoptosis of hematopoietic progenitor and stem cells, and elevated lethality after TBI compared to their counterparts.[78] Embryonic fibroblasts from the model mice expressed elevated levels of ROS at basal levels and after exposure to IR, correlating with increased apoptosis and decreased clonogenic survival.[80] In transgenic cells stably expressing GFP, steady synthesis and maturation of GFP and GFP redox cycling activity occur, causing increased formation ROS compared to the wild-type cells, leading to cytotoxicity and tissue abnormalities.[75] Increase in the steady state levels of ROS could cause activation of Bax and caspases, leading to induced apoptosis.[81] In this work, elevated level of both the percentage of cells expressing Bax and apoptotic cells was observed in the bone marrow from C57BL/6N-GFP mice compared to that in their wild type counterparts. These results indicated a causal connection between gene activation and apoptosis induction. These findings also suggested that the Bax/Bcl-2 switch was flipped in cells from C57BL/6N-GFP mice, possibly by increased ROS, to contribute to the induced apoptosis. Furthermore, increased ROS could activate multiple signal transduction pathways.[82] ROS stress itself may also increase the levels of other stress-inducible second messengers. As key signaling molecules, ROS play an important role in the progression of inflammatory disorders. Elevations in total leukocyte count, a reliable biomarker of inflammation, are significantly in response to inflammation.[83,84] Enhanced generation of ROS by polymorphonuclear neutrophils could cause endothelial dysfunction and tissue injury.[85] In fact, in our preliminary study on the total leukocyte count in peripheral blood histogram, no significant difference was found between C57BL/6N-GFP mice and C57BL/6N-WT mice at postnatal age of 6-8 weeks while the count was more than twice higher in C57BL/6N-GFP mice than that in their counterparts at postnatal age of 10 months (data not shown). These results suggested possible induction of chronic inflammation in C57BL/6N-GFP mice. Equally significant and interesting, many studies with *in vitro* and *in vivo* systems demonstrate enhanced ROS formation and altered responses of oxidative stress and inflammation genes of GFP transgenic cells and animals to cytotoxic or genotoxic insults including IR.[86] Thus, in the case of C57BL/6N-GFP mice exposed to TBI, GFP-induced ROS could be an agonist to IR-induced ROS, conveying more information transduced into the cell to activate pro-apoptotic and inflammatory responses, causing cellular damage triggering and enhancing induction of apoptosis, resulting in increased lethality to radiation-induced bone marrow death.

Although the exact mechanisms underlying altered response of GFP transgenic mice to IR warranted for further studies, it does not affect in any way the conclusion of the present work: enhanced expression of GFP in transgenic cells and animals is not innoxious and investigation using these organisms should be seriously taken into consideration in the study of radiation biology. In summary, although being not yet proven totally untrue, normalness and healthiness in physiological functioning and pathological responses of GFP transgenic cells and animals compared to their wild-type counterparts have certainly not been proven to be true. Under these circumstances, even taking into account the great achievements obtained by GFP transgenic technologies, it is non-negligible that application of GFP in life science research should be highly concerned.

Acknowledgments

The authors thank Ms. Hiromi Arai (QST-NIRS, Japan) for performing X-irradiations. The expert technical assistance and administrative support of Ms. Chiaki Suzuki, Mr. Wataru Ueno, Ms. Taeko Iwai, Ms. Sayaka Hayashi, Ms. Hiroko Nakamura, Mr. Sadao Hirobe, Ms. Mikiko Nakajima, Ms. Chianing Hsieh, Ms. Hiromi Arai and Ms. Yasuko Morimoto (QST-NIRS, Japan), are gratefully acknowledged. The authors also thank Prof. Xiaoqin Ye (The University of Georgia, USA), for her critical and constructive comments on analyzing the flow cytometric data. We are deeply grateful to Dr. Hiroko Ishii-Ohba and Dr. Masahiko Mori (QST-NIRS, Japan), for their continual encouragement and support. Thanks are also due to the anonymous peer reviewers for providing the constructive comments that strengthened the presentation of this work.

Declaration of Conflicting Interests

The author(s) declared no potential conflicts of interest with respect to the research, authorship, and/or publication of this article.

Funding

The author(s) disclosed receipt of the following financial support for the research, authorship, and/or publication of this article: The seventh author (Zeenath Fardous) was a fellow of the Nuclear Researchers Exchange Programme 2018 supported by the Ministry of Education, Culture, Sport, Sciences and Technology (MEXT), Japan, and the Nuclear Safety Research Association, Japan. This work was partially supported by JSPS KAKENHI 25340041, Japan.

ORCID iD

Takanori Katsube https://orcid.org/0000-0002-6374-4272
Bing Wang https://orcid.org/0000-0002-7180-639X

References

1. Shimomura O. Discovery of green fluorescent protein (GFP) (Nobel Lecture). *Angew Chem Int Ed Engl*. 2009;48(31): 5590-5602.
2. Sarkar P, Chattopadhyay A. GFP fluorescence: a few lesser-known nuggets that make it work. *J Biosci*. 2018;43(3):421-430.
3. Tsien RY. The green fluorescent protein. *Annu Rev Biochem*. 1998;67:509-544.
4. Godwin AR, Stadler HS, Nakamura K, Capecchi MR. Detection of targeted GFP-Hox gene fusions during mouse embryogenesis. *Proc Natl Acad Sci USA*. 1998;95(22):13042-13047.
5. Hadjantonakis AK, Macmaster S, Nagy A. Embryonic stem cells and mice expressing different GFP variants for multiple non-invasive reporter usage within a single animal. *BMC Biotechnol*. 2002;2:11.

6. Hadjantonakis AK, Nagy A. The color of mice: in the light of GFP-variant reporters. *Histochem Cell Biol*. 2001;115(1):49-58.
7. Berg RH, Beachy RN. Fluorescent protein applications in plants. *Methods Cell Biol*. 2008;85(chap 8):153-177.
8. Day RN, Schaufele F. Fluorescent protein tools for studying protein dynamics in living cells: a review. *J Biomed Optics*. 2008; 13(3):031202.
9. Detrich HW III. Fluorescent proteins in zebrafish cell and developmental biology. *Methods Cell Biol*. 2008;85(chap 10):219-240.
10. Wiedenmann J, Oswald F, Nienhaus GU. Fluorescent proteins for live cell imaging: opportunities, limitations, and challenges. *IUBMB Life*. 2009;61(11):1029-1042.
11. Sparkes I, Brandizzi F. Fluorescent protein-based technologies: shedding new light on the plant endomembrane system. *Plant J*. 2012;70(1):96-107.
12. Shorter SA, Pettit MW, Dyer PDR, et al. Green fluorescent protein (GFP): is seeing believing and is that enough? *J Drug Target*. 2017;25(9-10):809-817.
13. Saady A, Böttner V, Meng M, et al. An oligonucleotide probe incorporating the chromophore of green fluorescent protein is useful for the detection of HER-2 mRNA breast cancer marker. *Eur J Med Chem*. 2019;173:99-106.
14. Daian E Silva DSO, Pinho TMG, Rachid MA, Barbosa-Stancioli DF, Da Fonseca FG. The perennial use of the green fluorescent protein marker in a live vaccinia virus Ankara recombinant platform shows no acute adverse effects in mice. *Braz J Microbiol*. 2019;50(2):347-355.
15. Tanno Y, Kobayashi K, Tatsuka M, Gotoh E, Takakura K. Mitotic arrest caused by an X-ray microbeam in a single cell expressing EGFP-aurora kinase B. *Radiat Protect Dosi*. 2006;122(1-4): 301-306.
16. Aizawa K, Yori K, Kaminaga C, et al. Responses of embryonic germ cells of the radiation-sensitive Medaka mutant to gamma-irradiation. *J Radiat Res*. 2007;48(2):121-128.
17. Maruyama K, Iwanami N, Maruyama-Hayakawa T, Doi K, Wang B. A small fish model for quantitative analysis of radiation effects using visualized thymus responses in GFP transgenic medaka. *Int J Radiat Biol*. 2019;95(8):1144-1149.
18. Kimura H, Lee C, Hayashi K, et al. UV light killing efficacy of fluorescent protein-expressing cancer cells in vitro and in vivo. *J Cell Biochem*. 2010;110(6):1439-1446.
19. Baumstark-Khan C, Hellweg CE, Palm M, Horneck G. Enhanced green fluorescent protein (EGFP) for space radiation research using mammalian cells in the International Space Station. *Phys Med*. 2001;17(suppl 1):210-214.
20. Baumstark-Khan C, Hellweg CE, Arenz A, Meier MM. Cellular monitoring of the nuclear factor kappaB pathway for assessment of space environmental radiation. *Radiat Res*. 2005;164(4 pt 2): 527-530.
21. Petrova AS, Lukonina AA, Badun GA, Kudryasheva NS. Fluorescent coelenteramide-containing protein as a color bioindicator for low-dose radiation effect. *Anal Bioanal Chem*. 2017;409(18): 4377-4381.
22. Anaganti N, Basu B, Apte SK. In situ real-time evaluation of radiation-responsive promoters in the extremely radioresistant-microbe deinococcus radiodurans. *J Biosci*. 2016;41(2):193-203.
23. Zhang G, Gurtu V, Kain SR. An enhanced green fluorescent protein allows sensitive detection of gene transfer in mammalian cells. *Biochem Biophys Res Commun*. 1996;227(3):707-711.
24. Heim R, Prasher DC, Tsien RY. Wavelength mutations and post-translational autoxidation of green fluorescence protein. *Proc Natl Acad Sci USA*. 1994;91(26):12501-12504.
25. Okabe M, Ikawa M, Kominami K, Nakanishi T, Nishimune Y. 'Green mice' as a source of ubiquitous green cells. *FEBS Lett*. 1997;407(3):313-319.
26. Ansari AM, Ahmed AK, Matsangos AE, et al. Cellular GFP toxicity and immunogenicity: potential confounders in vivo cell tracking experiments. *Stem Cell Rev Rep*. 2016;12(5):553-559.
27. Huang WY, Aramburu J, Douglas PS, Izumo S. Transgenic expression of green fluorescence protein can cause dilated cardiomyopathy. *Nat Med*. 2000;6(5):482-483.
28. Li H, Wei H, Wang Y, Tang H, Wang Y. Enhanced green fluorescent protein transgenic expression in vivo is not biologically inert. *J Proteome Res*. 2013;12(8):3801-3808.
29. Avey SR, Ojehomon M, Dawson JF, Gillis TE. How the expression of green fluorescent protein and human cardiac actin in the heart influences cardiac function and aerobic performance in zebrafish Danio rerio. *J Fish Biol*. 2017;92(1):177-189.
30. Kam WW, Middleton R, Lake V, Banati RB. Green fluorescent protein alters the transcriptional regulation of human mitochondrial genes after gamma irradiation. *J Fluoresc*. 2013;23(4): 613-619.
31. Gau CD, Poljak A, Wasinger V, Roy P, Moens P. Green fluorescent protein expression triggers proteome changes in breast cancer cells. *Exp Cell Res*. 2014;320(1):33-45.
32. Liu HS, Jan MS, Chou CK, Chen PH, Ke NJ. Is green fluorescent protein toxic to the living cells? *Biochem Biophys Res Commun*. 1999;260(3):712-717.
33. Makanae K, Kintaka R, Makino T, Kitano H, Moriya H. Identification of dosage-sensitive genes in Saccharomyces cerevisiae using the genetic tug-of-war method. *Genome Res*. 2013;23(2): 300-311.
34. Wallace LM, Moreo A, Clark KR, Harper SQ. Dose-dependent toxicity of humanized renilla reniformis GFP (hrGFP) limits its utility as a reporter gene in mouse muscle. *Mol Ther Nucleic Acids*. 2013;2(4):e86.
35. Goto H, Yang B, Petersen D, et al. Transduction of green fluorescent protein increased oxidative stress and enhanced sensitivity to cytotoxic drugs in neuroblastoma cell lines. *Mol Cancer Ther*. 2003;2(9):911-917.
36. Nakanishi T, Kuroiwa A, Yamada S, et al. FISH analysis of 142 EGFP transgene integration sites into the mouse genome. *Genomics*. 2002;80(6):564-574.
37. Ikawa M, Kominami K, Yoshimura Y, Tanaka K, Nishimune Y, Okabe M. Green fluorescent protein as a marker in transgenic mice. *Dev Growth Differ*. 1995;37(4):455-459.
38. Yonezawa M, Misonoh J, Hosokawa Y.Two types of X-ray-induced radioresistance in mice: presence of 4 dose ranges with distinct biological effects. *Mutat Res*. 1996;358(2):237-243.
39. Shimomura O, Johnson FH, Saiga Y. Extraction, purification and properties of aequorin, a bioluminescent protein from the

luminous hydromedusan, *Aequorea. J Cell Comp Physiol*. 1962; 59(3):223-239.
40. Chalfie M, Tu Y, Euskirchen G, Ward WW, Prasher DC. Green fluorescent protein as a marker for gene expression. *Science*. 1994;263(5148):802-805.
41. Tanaka M, Kinoshita M, Kobayashi D, Nagahama Y.Establishment of Medaka (Oryzias latipes) transgenic lines with the expression of green fluorescent protein fluorescence exclusively in germ cells: a useful model to monitor germ cells in a live vertebrate. *Proc Natl Acad Sci U S A*. 2001;98(5):2544-2549.
42. Wang HJ, Lin AX, Zhang ZC, Chen YF. Expression of porcine growth hormone gene in transgenic rabbits as reported by green fluorescent protein. *Anim Biotechnol*. 2001;12(2):101-110.
43. Jensen DF, Schulz A. Exploitation of GFP-technology with filamentous fungi. In: Arora DK, Bridge PD, Bhatnagar D, eds. *Handbook of FungaI BiotechnoIogy*. Marcel Dekker; 2004: 439-449.
44. Chalfie M. GFP: Lighting up life. *Proc Natl Acad Sci U S A*. 2009; 106(25):10073-10080.
45. Dhungel B, Ohno Y, Matayoshi R, Otaki JM. Baculovirus-mediated gene transfer in butterfly wings in vivo: an efficient expression system with an anti-gp64 antibody. *BMC Biotechnol*. 2013;13:27.
46. Milesa EL, O'Gormana C, Zhao J, et al. Transgenic pig carrying green fluorescent proteasomes. *Proc Natl Acad Sci USA*. 2013; 110(16):6334-6339.
47. Crispo M, Vilariño M, dos Santos-Neto PC, et al. Embryo development, fetal growth and postnatal phenotype of eGFP lambs generated by lentiviral transgenesis. *Transgenic Res*. 2015; 24(1):31-41.
48. Kato H, Abe K, Yokota S, et al. Establishment of oct4: gfp transgenic zebrafish line for monitoring cellular multipotency by GFP fluorescence. *In Vitro Cell Dev Biol Anim*. 2015;51(1):42-49.
49. Yoshimura A, Kawamata M, Yoshioka Y, et al. Generation of a novel transgenic rat model for tracing extracellular vesicles in body fluids. *Sci Rep*. 2016;6:31172.
50. Seita Y, Tsukiyama T, Iwatani C, et al. Generation of transgenic cynomolgus monkeys that express green fluorescent protein throughout the whole body. *Sci Rep*. 2016;6:24868.
51. Ma DF, Sudo K, Tezuka H, et al. Polyclonal origin of hormone-producing cell populations evaluated as a direct in situ demonstration in EGFP/BALB/C chimeric mice. *J Endocrinol*. 2010;207(1): 17-25.
52. Nishimura R, Goto M, Sekiguchi S, Fujimori K, Ushiyama A, Satomi S. Assessment for revascularization of transplanted pancreatic islets at subcutaneous site in mice with a highly sensitive imaging system. *Transplant Proc*. 2011;43(9):3239-3240.
53. Nishimura R, Ushiyama A, Sekiguchi S, et al. Effects of glucagon-like peptide 1 analogue on the early phase of revascularization of transplanted pancreatic islets in a subcutaneous site. *Transplant Proc*. 2013;45(5):1892-1894.
54. Tsujigiwa H, Hirata Y, Katase N, et al. The role of bone marrow-derived cells during the bone healing process in the GFP mouse bone marrow transplantation model. *Calcif Tissue Int*. 2013; 92(3):296-306.
55. Yang C, Gu L, Deng D. Bone marrow-derived cells may not be the original cells for carcinogen-induced mouse gastrointestinal carcinomas. *PLoS One*. 2013;8(11):e79615.
56. Khalil HA, Lei NY, Nie W, et al. Primary myofibroblasts maintain short-term viability following submucosal injection in syngeneic, immune-competent mice utilizing murine colonoscopy. *PLoS One*. 2015;10(5):e0127258.
57. Gil-Sanchis C, Cervelló I, Khurana S, Faus A, Verfaillie C, Simón C. Contribution of different bone marrow-derived cell types in endometrial regeneration using an irradiated murine model. *Fertil Steril*. 2015;103(6):1596-1605.e1.
58. Cheng Z, Peng HL, Zhang R, Fu XM, Zhang GS. Rejuvenation of cardiac tissue developed from reprogrammed aged somatic cells. *Rejuvenation Res*. 2017;20(5):389-400.
59. Frueh FS, Später T, Lindenblatt N, et al. Adipose tissue-derived microvascular fragments improve vascularization, lymphangiogenesis, and integration of dermal skin substitutes. *J Invest Dermatol*. 2017;137(1):217-227.
60. Takabatake K, Tsujigiwa H, Song Y, et al. The role of bone marrow-derived cells during ectopic bone formation of mouse femoral muscle in GFP mouse bone marrow transplantation model. *Int J Med Sci*. 2018;15(8):748-757.
61. Später T, Frueh FS, Karschnia P, Menger MD, Laschke MW. Enoxaparin does not affect network formation of adipose tissue-derived microvascular fragments. *Wound Repair Regen*. 2018;26(1):36-45.
62. Frueh FS, Später T, Körbel C, et al. Prevascularization of dermal substitutes with adipose tissue-derived microvascular fragments enhances early skin grafting. *Sci Rep*. 2018;8(1):10977.
63. Morita-Takemura S, Nakahara K, Hasegawa-Ishii S, et al. Responses of perivascular macrophages to circulating lipopolysaccharides in the subfornical organ with special reference to endotoxin tolerance. *J Neuroinflammation*. 2019;16(1):39.
64. Olivieri G, Bodycote J, Wolff S. Adaptive response of human lymphocytes to low concentrations of radioactive thymidine. *Science*. 1984;223(4636):594-597.
65. United Nations Scientific Committee on the Effects of Atomic Radiation. Adaptive response to radiation in cells and organisms. In: United Nations Scientific Committee on the effects of Atomic Radiation, ed. *Sources and Effects of Ionizing Radiation: UNSCEAR Report to the General Assembly with Scientific Annexes*; 1994:185-272.
66. Varès G, Wang B, Tanaka K, Nakajima T, Nenoi M, Hayata I. Radiation-induced adaptive response with reference to evidence and significance: a review. *Indian J Radiat Res*. 2006;3(1):16-34.
67. Tapio S, Jacob V. Radioadaptive response revisited. *Radiat Environ Biophys*. 2007;46(1):1-12.
68. Nenoi M, Wang B, Vares G.In vivo radioadaptive response: a review of studies relevant to radiation-induced cancer risk. *Human Exp Toxicol*. 2015;34(3):272-283.
69. Yonezawa M, Misonoh J, Hosokawa Y. Acquired radioresistance after small dose X-irradiation in mice. *J Radiat Res*. 1990;31(3): 256-262.
70. Nose M, Wang B, Itsukaichi H, et al. Rescue of lethally irradiated mice from hematopoietic death by pre-exposure to 0.5 Gy X rays without recovery from peripheral blood cell depletion and its modification by OK432. *Radiat Res*. 2001;156(2):195-204.

71. Yonezawa M. Induction of radio-resistance by low dose X-irradiation. *Yakugaku Zasshi (in Japanese)*. 2006;126(10):833-840.
72. Otsuka K, Koana T, Tomita M, Ogata H, Tauchi H. Rapid myeloid recovery as a possible mechanism of whole-body radioadaptive response. *Radiat Res*. 2008;170(3):307-315.
73. Wang B, Tanaka K, Ninomiya Y, et al. Relieved residual damage in the hematopoietic system of mice rescued by radiation-induced adaptive response (Yonezawa effect). *J Radiat Res*. 2013; 54(1): 45-51.
74. Wang B, Tanaka K, Ninomiya Y, et al. Increased hematopoietic stem cells/hematopoietic progenitor cells measured as endogenous spleen colonies in radiation-induced adaptive response in mice (Yonezawa effect). *Dose Response*. 2018;16(3):155932581 8790152.
75. Ganini D, Leinisch F, Kumar A, et al. Fluorescent proteins such as eGFP lead to catalytic oxidative stress in cells. *Redox Biol*. 2017; 12:462-468.
76. Droge W. Free radicals in the physiological control of cell function. *Physiol Rev*. 2002;82(1):47-95.
77. Batandier C, Leverve X, Fontaine E. Opening of the mitochondrial permeability transition pore induces reactive oxygen species production at the level of the respiratory chain complex I. *J Biol Chem*. 2004;279(17):17197-17204.
78. Pawar SA, Shao L, Chang J, et al. C/EBPδ deficiency sensitizes mice to ionizing radiation-induced hematopoietic and intestinal injury. *PLoS One*. 2014;9(4):e94967.
79. Yazlovitskaya EM, Voziyan PA, Manavalan T, Yarbrough WG, Ivanova AV. Cellular oxidative stress response mediates radiosensitivity in Fus1-deficient mice. *Cell Death Dis*. 2015; 6(2): e1652.
80. Banerjee S, Aykin-Burns N, Krager KJ, et al. Loss of C/EBPδ enhances IR-induced cell death by promoting oxidative stress and mitochondrial dysfunction. *Free Radic Biol Med*. 2016;99: 296-307.
81. Zhou DR, Eid R, Boucher E, Miller KA, Mandato CA, Greenwood MT. Stress is an agonist for the induction of programmed cell death: a review. *Biochim Biophys Acta Mol Cell Res*. 2019; 1866(4):699-712.
82. Kiang JG, Olabisi AO. Radiation: a poly-traumatic hit leading to multi-organ injury. *Cell Biosci*. 2019;9:25.
83. Libby P. Inflammatory mechanisms: the molecular basis of inflammation and disease. *Nutr Rev*. 2007;65(12 pt 2):S140-146.
84. Chmielewski PP, Strzelec B. Elevated leukocyte count as a harbinger of systemic inflammation, disease progression, and poor prognosis: a review. *Folia Morphol*. 2018;77(2):171-178.
85. Mittal M, Siddiqui MR, Tran K, Reddy SP, Malik AB. Reactive oxygen species in inflammation and tissue injury. *Antioxid Redox Signal*. 2014;20(7):1126-1167.
86. Kalyanaraman B, Zielonka J.Green fluorescent proteins induce oxidative stress in cells: a worrisome new wrinkle in the application of the GFP reporter system to biological systems? *Redox Biol*. 2017;12:755-757.